Springer

Journal of Mechanical Science and Technology 23 (2009) 2424~2433

Journal of Mechanical Science and Technology

www.springerlink.com/content/1738-494x
DOI 10.1007/s12206-009-0627-6

Effects of surface geometry and non-newtonian viscosity on the flow field in arterial stenoses †

W. W. Jeong and K. Rhee*

Department of Mechanical Engineering, Myongji University,Yongin, 449-728, Korea

(Manuscript Received September 24, 2008; Revised May 7, 2009; Accepted May 15, 2009)

Abstract

Hemodynamics including flow pattern, shear stress, and blood viscosity characteristics has been believed to affect the development and progression of arterial stenosis, but previous studies lack of realistic physiological considerations such as irregular surface geometry, non-Newtonian viscosity characteristics and flow pulsatility. The effects of surface irregularities and non-Newtonian viscosity on flow fields were explored in this study using the arterial stenosis models with 48% arterial occlusions under physiological flow condition. Computational flow dynamics based on the finite volume method was employed for Newtonian and non-Newtonian fluid. The wall shear stresses (WSS) in the irregular surface model were higher compared to those in the smooth surface models. Also, non-Newtonian viscosity characteristics increase the peak WSS significantly. The dimensionless pressure drop and the time averaged WSS in pulsatile flow were higher than those in steady flow. But pulsatility effects on pressure and WSS were less significant compared to non-Newtonian viscosity effects. Therefore, irregular surface geometry and non-Newtonian viscosity characteristics should be considered in predicting pressure drop and WSS in stenotic arteries.

Keywords: Coronary stenosis; Pulsatile flow; Rheological characteristics; Atherosclerosis; Wall shear stress

1. Introduction

Atherosclerosis is a focal pathological phenomenon characterized by thickening and hardening of arteries due to deposits, such as lipids, carbohydrates, blood products, fibrous tissue, and the asymptomatic coronary atherosclerotic lesions are common in industrialized society's denizens. Progression of these lesions result in thrombotic complications such as cardiac arrest and stroke which cause high mortality and morbidity [1, 2]. Hemodynamics including flow pattern [3], shear stress, and blood viscosity characteristics [4, 5] affect the development and progression of arterial stenosis. Pressure drop and wall shear stress (WSS) distribution in the stenosis is particularly important since pressure drop is related to the cardiac afterload. Increased heart afterload is related to the development of hypertension and the hypertrophy of ventricles. Also, the arterial wall shear stress is related to the function of the endothelium. It has been believed that low and oscillatory shear stress enhances lipid transport across the endothelium, which is an important process in the early stage of atherosclerosis. Also, high wall shear stress on the stenotic region may cause endothelium disruption and hemolysis. Therefore, fluid mechanical analysis in the arterial stenosis can help researchers understood the hemodynamic environment of arterial disease progression.

Analyzing fluid mechanics inside the arterial tree is a formidable work because of complex vessel geometry, moving arterial wall, pulsatile flow and non-Newtonian viscosity. Rapid growth of computer hardware and software technology during the last two decades has given leeway to computational fluid dynamics (CFD) in the biological system; therefore, experimentally impossible and complex problems can

† This paper was recommended for publication in revised form by Associate Editor Yang Na

*Corresponding author. Tel.: +82 31 330 6426, Fax.: +82 31 330 6957
E-mail address: khanrhee@mju.ac.kr

be analyzed numerically without significant effort and cost. After the initial numerical study on the hemodynamic characteristics in a stenotic artery by Young [6], many researchers (Forrester and Young, Morgan and Young, Lee and Fung, Deshpande *et al.*, Johnson and Kilpatrick) [7-11] have studied the hemodynamics of a stenotic artery by modeling the stenotic lumen geometry using a smooth curve such as a cosine. But, the lumen of a stenotic artery is not smooth and it is composed of many small valleys and ridges.

Previously, Back *et al.* [3, 12, 13] experimentally measured the pressure drop and wall shear stress in an irregular shape stenotic model using the left circumflex coronary artery casting of a man. The results of this study showed that the effect of irregular surfaces - small scale valleys and ridges along the stenotic vessel wall - led to the sharp spikes of wall shear stresses for Reynolds numbers from 60 to 500. Based on Back *el a.l*'s experiment, Johnston and Kilpatrick [14] presented a numerical study about three stenosis shapes (cosine, irregular, smooth) by using a commercial CFD package. They calculated the pressure drop and the wall shear stress of stenotic region for different Reynolds numbers (between 20 and 1000) in steady flow. Andersson *et al* [16] concretized the study of Johnston and Kilpatrick [14], and showed that the surface irregularities did not affect the flow resistance at low Reynolds numbers, while wall shear stress was larger in the irregular surface model at high Reynolds numbers. Yakhot *et al.* [17] measured the pressure drop and the wall shear stress in the stenotic region for different Reynolds numbers by using IB (Immersed Boundary) method suggested by Peskin [18], and also analyzed the streamlines in the stenotic region. This study also included the effects of pulsatile flow by using a sinusoidal flow waveform. The result showed that the surface irregularities had no significant influence on the flow resistance across an obstacle for the physiological range of Reynolds numbers. Chakravarty *et al.* [15, 19] calculated the pressure gradient, the wall shear stress and velocity profile of a stenotic region under unsteady pulsatile flow by applying time varying inlet boundary condition using a body acceleration waveform. This study was performed by using non-uniform, non-staggered grid, and the effect of surface irregularities on the flow velocity, the flux, the resistive impedance and the wall shear stress were explored.

Newtonian viscosity characteristics were assumed in most previous hemodynamic studies of stenotic arteries. But blood is a non-Newtonian fluid that shows shear-dependent viscous properties because of its nonhomogeneous nature in micro scale. Blood contains blood elements such as erythrocytes, leukocytes, and platelets in blood plasma. The apparent viscosity increases at low shear rates, and has a constant value for the high shear rates. Strain rate variation is significant in the disturbed flow region in the stenosis, and the effect of non-Newtonian viscosity on the shear stress in atherosclerotic coronary arteries could be more significant than that in non-diseased ones. Non-Newtonian viscosity might affect the pressure drop, shear rate and stress, and flow characteristics, but the effects of non-Newtonian viscosity have not been fully considered in analyzing the flow fields in a stenotic coronary artery under physiological blood flow waveform.

Therefore, we would like to consider the effects of lumen surface irregularity, physiological flow waveform and non-Newtonian viscosity characteristics in a stenotic artery using a numerical method. Three different shapes of stenosis models (cosine, irregular, smooth) were used in order to investigate surface irregularity effect of the stenotic regions.

2. Methods

2.1 Stenosis models

The mild arterial stenosis models used in this study were based on the vascular axisymmetric replica of the segment of a circumflex coronary artery which was used by Back *et al.* [13]. The three different stenosis models (irregular, cosine, smooth) shown Fig. 1 were simulated. They had 48% areal occlusions and thus classified as mild stenosis. The first model (irregular) was the straight axisymmetric model of Back *et al.* [13], which mimicked real surface irregularities, since the actual axial variation of the cross-sectional area of a left circumflex coronary artery was retained from the cast of a human cadaver. The second model (cosine) had the stenotic shape of a cosine curve.

$$R(z,t)=\begin{cases} r_0-\dfrac{\delta}{2}\left[1+\cos\left\{\pi\left(z-z_1\right)/z_0\right\}\right] \\ \qquad d\le z\le d+2z_0 \\ r_0 \end{cases} \tag{1}$$

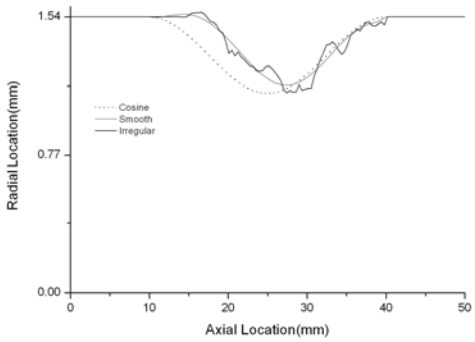

Fig. 1. Lumen geometry of the stenotic region of irregular, cosine and smooth arterial model.

The radius(R) in the stenotic region was given as a cosine function suggested by Young [6], where z_0 was the half length of a stenotic region, δ was the maximum width of the stenosis and z_1 was the center of the stenosis with $\delta = 0.276R_0$ (R_0 being the unconstructed radius of the stenosed vessel). The third model (smooth) had a stenosis shape which was given by a smooth curve fitted to the first irregular stenosis model. Three stenosis models were analyzed in order to observe the effects of the surface geometrical irregularity of a stenotic artery on the pressure drops and wall shear stresses.

2.2 Governing equation

The numerical fluid mechanical study for the stenosis model was based on the continuity and momentum equations. Continuity equation was expressed as:

$$\frac{\partial \rho}{\partial t} + \nabla \bullet (\rho \vec{v}) = 0 \tag{2}$$

For 2D axisymmetric geometries, the continuity equation was given by

$$\frac{\partial \rho}{\partial t} + \frac{\partial}{\partial x}(\rho v_x) + \frac{\partial}{\partial r}(\rho v_r) + \frac{\rho v_r}{r} = 0 \tag{3}$$

Where x is the axial coordinate, r is the radial coordinate, v_x is the axial velocity, and v_r is the radial velocity. Momentum equation is expressed as:

$$\frac{\partial \rho}{\partial t}(\rho \vec{v}) + \nabla \bullet (\rho \vec{v}\vec{v}) = -\nabla p + \nabla \bullet \left(\overline{\overline{\tau}}\right) + \rho \vec{g} \tag{4}$$

Where p is the static pressure, $\overline{\overline{\tau}}$ is the stress tensor, and $\rho\vec{g}$ and $\vec{F}$ are the gravitational body force and external body force, respectively.

The stress tensor $\overline{\overline{\tau}}$ was given by

$$\overline{\overline{\tau}} = \eta\left[\left(\nabla\vec{v} + \nabla\vec{v}^T\right) - \frac{2}{3}\nabla \bullet \vec{v} I\right] \tag{5}$$

Where η is the molecular viscosity, I is the unit tensor, and the second term on the right hand side is the effect of volume dilation which is zero for incompressible flow.

For 2D axisymmetric geometries, the axial and radial momentum equations are given by

$$\begin{aligned}&\frac{\partial}{\partial t}(\rho v_x) + \frac{1}{r}\frac{\partial}{\partial x}(r\rho v_x v_x) + \frac{1}{r}\frac{\partial}{\partial r}(r\rho v_r v_x)\\ &= -\frac{\partial p}{\partial x} + \frac{1}{r}\frac{\partial}{\partial x}\left[r\mu\left(2\frac{\partial v_x}{\partial x} - \frac{2}{3}(\nabla \bullet \vec{v})\right)\right]\\ &\quad + \frac{1}{r}\frac{\partial}{\partial r}\left[r\mu\left(2\frac{\partial v_x}{\partial r} + \frac{\partial v_r}{\partial x}\right)\right] + F_x\end{aligned} \tag{6}$$

And

$$\begin{aligned}&\frac{\partial}{\partial t}(\rho v_r) + \frac{1}{r}\frac{\partial}{\partial x}(r\rho v_r v_r) + \frac{1}{r}\frac{\partial}{\partial r}(r\rho v_r v_x)\\ &= -\frac{\partial p}{\partial r} + \frac{1}{r}\frac{\partial}{\partial x}\left[r\mu\left(\frac{\partial v_r}{\partial x} + \frac{\partial v_x}{\partial r}\right)\right]\\ &\quad + \frac{1}{r}\frac{\partial}{\partial r}\left[r\mu\left(2\frac{\partial v_r}{\partial r} - \frac{2}{3}(\nabla \bullet \vec{v})\right)\right]\\ &\quad - 2\mu\frac{v_r}{r^2} + \frac{2}{3}\frac{\mu}{r}(\nabla \bullet \vec{v}) + \rho\frac{v_z^2}{r} + F_r\end{aligned} \tag{7}$$

where $\nabla \bullet \vec{v} = \frac{\partial v_x}{\partial x} + \frac{\partial v_r}{\partial r} + \frac{v_r}{r}$ and v_z was the swirl velocity.

2.3 Numerical method

The governing equations were solved numerically by using the commercial CFD code (FLUENT) based on the finite volume method. Pressure-based implicit solver, first order upwind scheme for spatial discretization, and SIMPLE/PISO scheme for pressure and velocity coupling were used. Time step size was 0.03 sec and solution converged within 50 iterations per a time step. The vessel diameter and vessel length for three stenosis models were 3.08 mm and of 50 mm, respectively. Flow outlet boundary condition was given for the outlet. The flow field changes were not

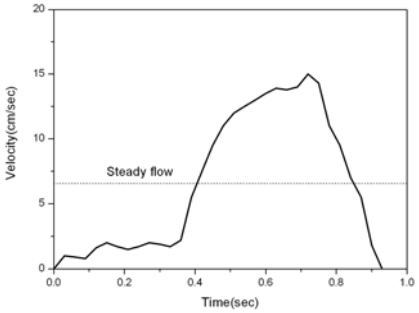

Fig. 2. Physiological velocity waveform of the left circumflex coronary artery used in this study [20].

significant in streamwise direction near the exit region of the calculation domain. Streamwise pressure gradient was negligible near the exit boundary. Further increase of the calculation domain in the distal streamwise direction did not change the calculation results. The model was composed of about 12,000 quadrilateral cells. One period of flow waveform was divided (Fig. 2) into 32 intervals, and the uniform inlet velocity profile was updated at each interval. The magnitude of the inlet velocity of steady flow was calculated from the time-averaged mean velocity of physiological pulsatile flow. The flow waveform shown in Fig. 2 was obtained from the blood flow waveform in a left circumflex coronary artery [20].

For Newtonian fluid, viscosity of 0.003 kg/m·s^2 and density of 1055kg/m^3 were used. The non-Newtonian viscosity characteristic of blood was incorporated by using the Carreau model [5, 24]. The equation for the Carreau model was expressed as:

$$\eta = \eta_\infty + (\eta_0 - \eta_\infty)\left[1 + \lambda^2\gamma^2\right]^{\left(\frac{q-1}{2}\right)} \quad (8)$$

where η is viscosity and γ is shear rate. The rheological parameters for human blood are as follows: η_0 = 0.056Pa·s, η_∞ = 0.00345Pa·s, λ = 3.313s, q= 0.356.

3. Results

We simulated the flow fields of the stenotic regions for three different stenosis models as shown in Fig. 1. The pressure, wall shear stress and velocity profiles in the stenotic region for both Newtonian and non-Newtonian flow were calculated. Our numerical scheme was validated for the steady flow case by comparing the calculated results to the previous worker's experimental data. The numerical solutions of the flow fields under the physiological flow waveforms were calculated, and the effects of surface irregularity and non-Newtonian viscosity on flow fields were investigated.

3.1 Model validation

To validate our numerical scheme, the calculation results were compared with the experimental results of Back *et al,* [13]. The pressure drop was normalized by dynamic pressure based on the areal mean velocity (u_0), and the distribution is shown in Fig. 3. The peak wall shear stresses and overall pressure drops of the calculated and experimental results for the irregular stenosis model are shown in Figs. 4 and 5. CFD solutions agreed well with the experimental data, which implied that our numerical scheme was as good as those of previous workers [11, 14, 15].

Fig. 3 shows that the dimensionless pressure drops were larger for the lower Reynolds numbers than those for the higher Reynolds numbers in steady flow condition. Figs. 4 and 5 suggest that the peak wall shear stress and pressure drop increased with the increase in Reynolds number. Fig. 6 shows the calculated viscosity by using the Carreau model and the experimentally measured blood viscosity for different shear rates [5]. The results showed that the Carreau model correctly represented non-Newton viscosity behavior of blood.

3.2 Pressure drop

Pressures at different axial locations were normalized by the mean velocity (u_0), which was the areal mean velocity of steady flow. Temporally averaged pressures were used at each axial location for pulsatile flow. Normalized pressure drops are shown in Fig. 7 for the Newtonian and non-Newtonian flow. Normalized mean pressure drops in pulsatile flow were greater than those in steady flow at all axial locations for both Newtonian and non-Newtonian fluid. Larger pressure drops in pulsatile flow were observed for all three stenosis models. Normalized pressure drops in non-Newtonian fluid were larger than those in Newtonian fluid (Fig. 7). The effects of stenosis shape did not affect the normalized pressure drops significantly, but pressure drop was the largest in the cosine shape stenosis model. Pressure recovery was observed all different stenosis models

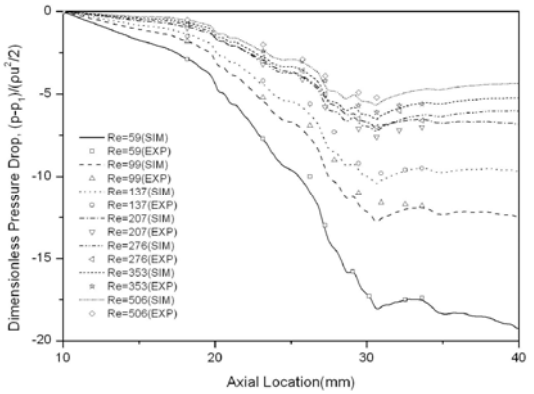

Fig. 3. Comparison of experimental and simulation results of dimensionless pressure drop at stenotic locations in steady flow.

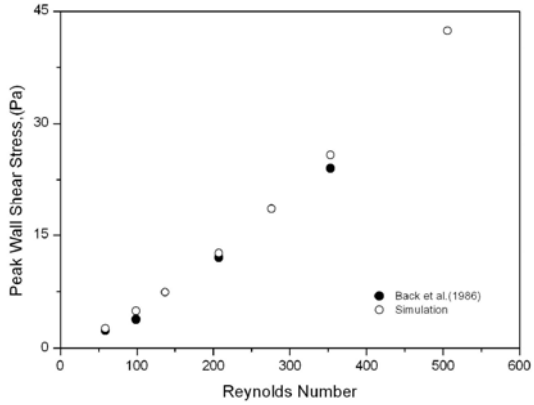

Fig. 4. Comparison of experimental and simulation results of peak wall shear stress at different Reynolds numbers in steady flow.

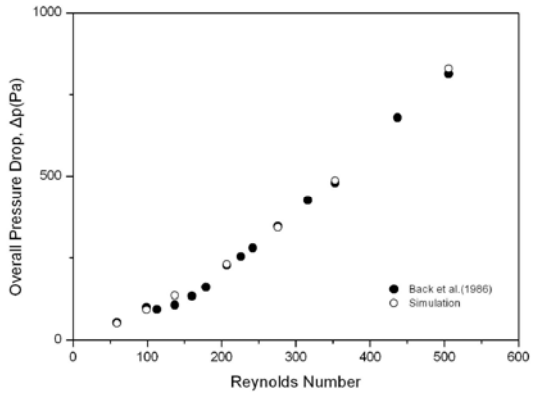

Fig. 5. Comparison of experimental and simulation results of overall pressure drops in the stenotic region at different Reynolds numbers in steady flow.

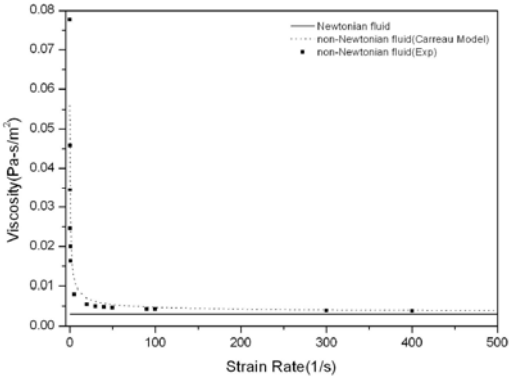

Fig. 6. Comparison of viscosity characteristics of Carreau model and human blood [5].

in Newtonian and non-Newtonian fluid. Pressure variation in the streamwise direction was negligible at axial locations downstream of 40 mm axial position.

3.3 Wall Shear Stress (WSS)

WSS is an important hemodynamic parameter in analyzing blood flow in arteries because it affects thickening of arterial wall and rupture of atherosclerotic plaque by influencing endothelial cell function. WSS is affected by the geometry of stenotic regions as well as rheological viscosity characteristics. Therefore, we calculated the WSS distributions for different stenosis models considering non-Newtonian viscosity characteristics. The WSS (τ_w) is modeled based on the Newton's viscosity law with shear dependant viscosity coefficient using Carreau's model:

$$\tau_w = \mu \cdot \dot{\gamma}_w \tag{9}$$

where μ is the shear dependent dynamic viscosity coefficient and $\dot{\gamma}_w$ is the wall shear rate.

Fig. 8 shows dimensionless WSS distributions for the three stenosis models. For pulsatile flow, wall shear stress at all axial locations was time averaged for a flow cycle and non-dimensionalized by areal averaged velocity at mean flow rate. The results showed that WSS distributions were similar for the cosine and smooth shapes stenosis model, but WSS distributions showed abrupt peaks and valleys for the irregular shape stenosis model. WSS was larger for non-Newtonian fluid compared to Newtonian fluid for the period of a flow cycle in all models. Irregular peaks of WSS were observed in the irregular stenosis model and the peak dimensionless WSS was about

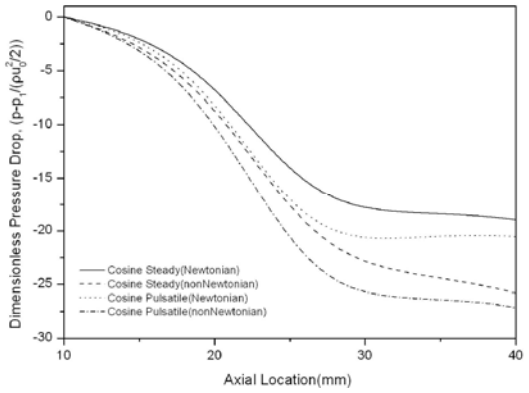

(a)

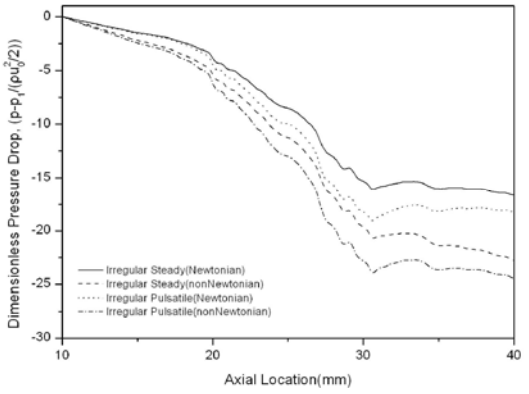

(b)

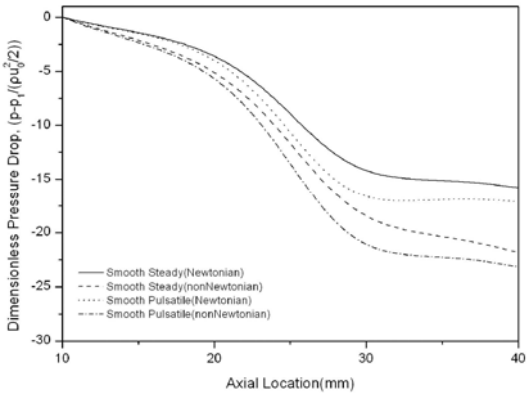

(c)

Fig. 7. Comparison of dimensionless pressure drop at steady flow and physiological pulsatile flow for Newtonian viscosity and non-Newtonian viscosity model. (a) cosine shape stenosis, (b) irregular shape stenosis, (c) smooth shape stenosis.

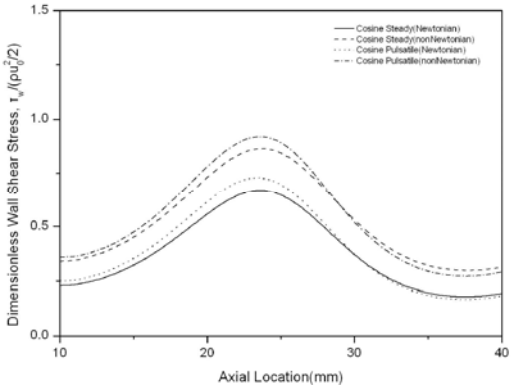

(a)

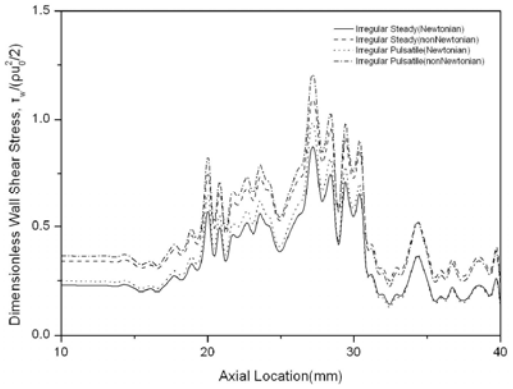

(b)

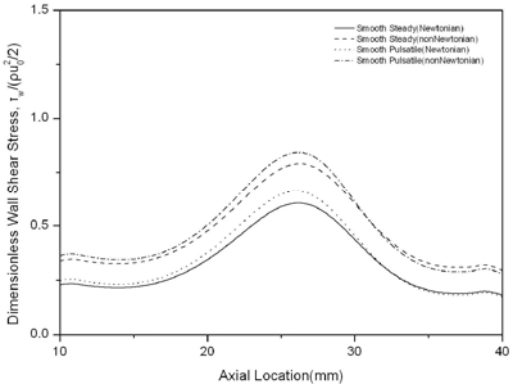

(c)

Fig. 8. Comparison of dimensionless wall shear stress at steady flow and physiological pulsatile flow for Newtonian viscosity and non-Newtonian viscosity model. (a) cosine shape stenosis, (b) irregular shape stenosis, (c) smooth shape stenosis.

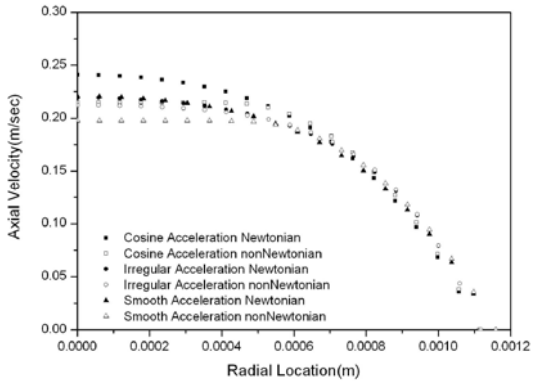

(a)

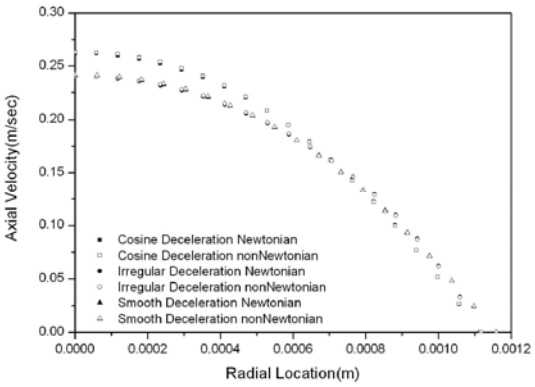

(b)

Fig. 9. Comparison of axial velocity profiles at acceleration phase and deceleration phase at the neck of the stenosis in three different models. (a) axial velocity of acceleration phase (t=0.42sec) in Newtonian fluid and non-Newtonian fluid, (b) axial velocity deceleration phase (t=0.84sec) in Newtonian fluid and non-Newtonian fluid.

30% higher compared to those of the cosine and the smooth stenosis model. Axial variation of WSS distribution was more significant in the irregular model.

3.4 Velocity profiles

We considered the axial velocity profiles at the neck of the stenosis (minimum lumen diameter) of three different stenoses. The axial velocity profiles at the acceleration phase (t=0.42sec) and deceleration phase (t=0.84sec) of three models are shown in Fig. 9. They showed that axial velocity profiles at the neck of the stenosis for non-Newtonian fluid were a little more blunt than those for Newtonian fluid at the acceleration phase (t=0.42sec), while the viscosity characteristics did not affect the velocity profile significantly at the deceleration phase (t=0.84sec). The velocity profiles were less blunt at the acceleration phase for Newtonian fluid. The centerline velocities for Newtonian fluid were slightly larger than those for non-Newtonian fluid at acceleration phase in all stenosis models, while the centerline velocities in Newtonian and non-Newtonian fluid were similar in all stenosis models at deceleration phase. The axial velocities at the constricted site (neck) were higher in the cosine shape model compared to those of other models.

4. Discussion

Blood flow within the arterial system affects the initiation and progression of vascular diseases [3-5, 13, 19, 25, 26], and arterial fluid mechanics is influenced by various physical parameters such as geometry, viscosity characteristics, wall elasticity and flow waveforms. We have studied the effects of stenosis geometry, non-Newtonian viscosity and flow pulsatility on the important hemodynamic parameters – pressure drop and WSS. Pressure drop determines heart afterload, WSS affects endothelium function and flow pattern determines the transport of blood born particles. We solved the physical governing equations incorporating a non-Newtonian viscosity model for the three different shapes of stenosis models under physiological flow condition.

To validate our numerical scheme, we compared our simulation results with the experimental results of Back *et al* [13]. Pressure drops and peak WSS in simulation results agreed well with the experimental results in steady flow. We calculated the pressure drops, WSS and velocity profiles for the three different stenosis models under physiological flow waveform. The results showed that pressure drops in the cosine shaped model was a little larger than those in the other shapes, but the differences were not significant. Pressure drops in non-Newtonian fluid model were larger compared to the Newtonian flow model.

Chakravarty *et al.* [15, 19] and Yakhot *et al.* [17] mentioned the effects of unsteady flow in the stenotic flow region, but simple waveforms, such as sinusoidal waveform or body acceleration waveform, were applied. In this study, we calculated hemodynamic parameters for both steady and physiological flow waveforms. Higher values of pressure drops and WSS at pulsatile flow were observed compared to those at steady flow. Also, it was shown that flow dynamics in

the irregular shaped model was significantly different from that in the smooth model. The effects of non-Newtonian fluid were also more significant in the irregular shaped model. Our simulation results were similar to those of the previous works in steady flow - pressure drops and WSS for non-Newtonian flow were greater than those for Newtonian flow [3, 4, 26, 27]. Also, the effects of non-Newtonian viscosity on pressure drop and WSS were more significant in pulsatile flow. Therefore, considering realistic hemodynamic factors such as non-Newtonian viscosity and physiological flow waveform could increase the pressure drop. This result implied that the assumption of neglecting non-Newtonian viscosity and pulsatility caused underestimation of heart afterload.

The wall shear stresses in the irregular shape model were higher compared to those in other models. This result was similar to the previous researcher's results using a simple sine flow waveform [17]. The WSS in the distal stenotic region was lower compared to proximal stenotic region. This result implied that blood borne particles could be accumulated in the distal stenotic region. Also, non-Newtonian viscosity characteristics increased the peak WSS significantly. Pulsatile flow also increased the WSS, but the pulsatility effects were less significant compared to non-Newtonian viscosity effects. High wall shear stress and low wall shear stress in the stenotic region may be related to the growth and the rupture of artheroma. The correlations between low and oscillatory WSS and atheroma formation have been reported. The roles of WSS of regulating endothelial function and structure, modulating endothelial gene expression [28], modifying bulk transport of lipid [29, 32], and enhancing monocyte adhesion to the endothelium [30, 31] have been investigated, but have not been fully understood yet. High WSS could injure the fibrous cap of atherosclerotic plaque and influence rupture of plaque.

In conclusion, this study indicates that irregular geometry, physiological flow waveform and non-Newtonian viscosity characteristics affect hemodynamic parameters, such as pressure drop, wall shear stress and velocity profile. Since non-Newtonian viscosity, flow pulsatility and irregular geometry increase the peak WSS in the simulation results, a more atherosclerosis susceptible (prone) hemodynamic environment is provided if we consider realistic hemodynamic conditions. Therefore, irregular surface geometries and non-Newtonian viscosity characteristics should be considered in predicting the pressure drop and WSS in stenotic arterial hemodynamic study.

References

[1] V. Fuster, L. Badimon, J. J. Badimon and J. H. Chesebro, The pathogenesis of coronary artery disease and the acute coronary syndromes: part 1, *New Engl. J. Med.* 326(4) (1992) 242-250.

[2] V. Fuster, L. Badimon, J. J. Badimon and J. H. Chesebro, The pathogenesis of coronary artery disease and the acute coronary syndromes: part 2*, New Engl. J. Med.* 326(5) (1992) 310-318.

[3] L. H. Back, Y. I. Cho, D. W. Crawford and R. F. Cuffel, Effect of mild atherosclerosis on flow resistance in a coronary artery casting of man, *J. Biomech. Eng.* 106 (1984) 48-53.

[4] R. C. Becker, The role of blood viscosity in the development and progression of coronary artery disease*, CCJM* 60 (1993) 353-358.

[5] Y. I. Cho and K. R. Kensey, Effects of the non-Newtonian viscosity of blood on flows in a diseased arterial vessel. Part 1: steady flows, *Biorheology*, 28 (1991) 241-262.

[6] D. F. Young, Effect of a time-dependent stenosis on flow through a tube, *J. Eng. Industries, ASME*, 90 (1968) 248-254.

[7] J. H. Forrester and D. F. Young, Flow through a converging-diverging tube and its implications in occlusive vascular disease-1: theoretical development, *J. Biomechanics*, 3 (1970) 297-305.

[8] B. Morgan and D. Young, An integral method for the analysis of flow in arterial stenoses, *Bull. Math. Biol.* 36 (1974) 39-53.

[9] J. S. Lee and Y. C. Fung, Flow in locally constricted tubes at low Reynolds numbers, *J. Appl. Mech.* 37 (1970) 9-16.

[10] M. Deshpande, D. Giddens and R. Mabon, Steady flow through modeled vascular stenoses, *J. Biomechanics*, 9 (1976) 165-174.

[11] P. R. Johnston and D. Kilpatrick, A mathematical model of paired arterial stenoses, *Computers in Cardiology* (Edited by Ripley, K.) (1990) pp. 229-232, IEEE Computer Society Press, Chicago.

[12] Y. I. Cho, L. H. Back, D. W. Crawford and R. F. Cuffel, Experimental study of pulsatile and steady flow through a smooth tube and an atherosclerotic coronary artery casting of man, *J. Biomechanics*, 16 (1983) 933-946.

[13] L. H. Back, J. R. Radbill, Y. I. Cho and D. W.

Crawford, Measurement and prediction of flow through a replica segment of a mildly atherosclerotic coronary artery of man, *J. Biomechanics*, 19 (1986) 1-17.

[14] P. R. Johnston and D. Kilpatrick, Mathematical modeling of flow through an irregular arterial stenosis, *J. Biomechanics*, 24 (1991) 1069-1077.

[15] S. Chakravarty and A. K. Sannigrahi, Effect of body acceleration on blood flow in irregular stenosed artery, *Mathl. Comput. Modelling*, 19 (1994) 93-103.

[16] H. I. Andersson, R. Halden and T. Glomsaker, Effects of surface irregularities on flow resistance in differently shaped arterial stenoses, *J. Biomechanics*, 33 (2000) 1257-1262.

[17] A. Yakhot, L. Grinberg and N. Nikitin, Modeling rough stenoses by an immersed-boundary method, *J. Biomech. Eng.* 38 (2005) 1115-1127.

[18] C. S. Peskin, Flow patterns around heart valves: a numerical method, *J. Computational Physics*, 10 (1971) 252-271.

[19] S. Chakravarty, P. K. Mandal and Sarifuddin, Effect of surface irregularities on unsteady pulsatile flow in a compliant artery, *Int. J. Non-Linear Mech.* 40 (2005) 1268-1281.

[20] S. Jin, Y. Yang, J. Oshinski, A. Tannenbaum, J. Gruden and D. Giddens, Flow pattern and wall shear stress distributions at atherosclerotic-prone sites in human left coronary artery-An exploration using combined methods of CT and computational fluid dynamics, *Proceedings of the 26th Annual International Conference of the IEEE EMBS* (2004) 3789-3791.

[21] L. H. Back, Theoretical investigation of mass transport to arterial walls in various blood flow regions, Part 1: Flow field and lipoprotein transport, Part 2: oxygen transport and its relationship to lipoprotein accumulation, *Mathl. Biosci*. 27 (1975) 231-262; 263-285.

[22] R. J. Lutz, J. N. Cannon, K. B. Bischoff, R. L. Dedrich, R. K. Stiles and D. L. Fry, Wall shear stress distribution in a model canine artery during steady flow, *Circ. Res*., 41 (1977) 391-399.

[23] M. K. Kolandavel, E. T. Fruend, S. Ringgaard and P. G. Walker, The effect of time varying curvature on species transport in coronary artery, *Annals Biomed. Eng.* 34 (2006) 1820-1832.

[24] R. K. Banerjee, A study of pulsatile flows with non-Newtonian viscosity of blood in large arteries, Ph.D. Thesis, Drexel University, Philadelphia, PA, (1992).

[25] A. G. Zaman, G. Helft, S. G. Worthley and J. J. Badimon, The role of plaque rupture and thrombosis in coronary artery disease, *Atherosclerosis*, 149 (2000) 251-266.

[26] B. M. Johnston, P. R. Johnston, S. Corney and D. Kilpatrick, Non-Newtonian blood flow in human right coronary arteries: steady state simulations, *J. Biomechanics.* 37 (2004) 709-720.

[27] J. V. Soulis, G. D. Giannoglou, Y. S. Chatzizisis, K. V. Seralidou, G. E. Parcharidis and G. E. Louridas, Non-Newtonian models for molecular viscosity and wall shear stress in a 3D reconstructed human left coronary artery, *Med. Eng. & Physics*, 30 (2008) 9-19.

[28] T. Nagel, N. Resnick, C. F. Dewey, Jr. and M. A. Gimbrone, Jr., Vascular endothelial cells respond to spatial gradients in fluid shear stress by enhanced activation of transcription factors, Arterioscler. *Thromb. Vasc. Biol*., 19 (1999) 1825-1834.

[29] A. Cho, L. Mitchell, D. Koopmans and B. L. Langille, Effects of changes in blood flow rate on cell death and cell proliferation in carotid arteries of immature rabbits, *Circ. Res.,* 81 (1997) 328-337.

[30] X. Deng, P. W. Stroman and R. Guidoin, Theoretical modeling of the release rate of low-density lipoproteins and their breakdown products at arterial stenoses, *Clin. Invest. Med*., 19 (1996) 83-91.

[31] S. Mohan, N. Mohan, A. J. Valente and E. A. Sprague, Regulation of low shear flow-induced HAEC VCAM-1 expression and monocyte adhesion, *Am. J. Physiol*., 276 (1999) C1100-C1107.

[32] C. G. Caro, J. M. Fitz-Gerald and R. C. Schroter, Atheroma and arterial wall shear. Observation, correlation and proposal of a shear dependent mass transfer mechanism for atherogenesis, *Proc. R. Soc. Lond. B. Biol. Sci.*, 177 (1971) 109-159.

[33] FLUENT INC, FLUENT 6.3 USER GUIDE (2006).

Kyehan Rhee received his B.S. in Mechanical Engineering from Seoul National University, Korea, in 1984. He then received his M.S. and Ph.D. degrees from Univ. of Minnesota in 1986 and 1990, respectively. Dr. Rhee is currently a Professor at the Department of Mechanical Engineering at

Myongji University in Yongin, Korea. His research interests include hemodynamics, blood flow in arteries, flow visualization, cellular/tissue response of hemodynamics stress, microfluidics and the development of intravascular treatment.

Woo-Won Jeong received his B.S. in Mechanical Engineering from Myongji University, Korea, in 2002. He then received his M.S. and Ph.D. degrees from Myongji Univ. in 2004 and 2009, respectively. Dr. Jeong is currently a Postdoc at the Department of Mechanical Engineering at Myongji University in Seoul, Yongin. His research interests include hemodynamics, blood flow in arteries, analysis of microscale fluid flow and fluid interaction with the biological environment.